Geiger-mode operation of ultraviolet avalanche photodiodes grown on sapphire and free-standing GaN substrates

E. Cicek, Z. Vashaei, R. McClintock, C. Bayram, and M. Razeghi[a)]
Department of Electrical Engineering and Computer Science, Center for Quantum Devices, Northwestern University, Evanston, Illinois 60208, USA

(Received 18 May 2010; accepted 7 June 2010; published online 1 July 2010)

GaN avalanche photodiodes (APDs) were grown on both conventional sapphire and low dislocation density free-standing (FS) c-plane GaN substrates. Leakage current, gain, and single photon detection efficiency (SPDE) of these APDs were compared. At a reverse-bias of 70 V, APDs grown on sapphire substrates exhibited a dark current density of 2.7×10^{-4} A/cm^2 whereas APDs grown on FS-GaN substrates had a significantly lower dark current density of 2.1×10^{-6} A/cm^2. Under linear-mode operation, APDs grown on FS-GaN achieved avalanche gain as high as 14 000. Geiger-mode operation conditions were studied for enhanced SPDE. Under front-illumination the 625-μm^2-area APD yielded a SPDE of ~13% when grown on sapphire substrates compared to more than 24% when grown on FS-GaN. The SPDE of the same APD on sapphire substrate increased to ~30% under back-illumination—the FS-GaN APDs were only tested under front illumination due to the thick absorbing GaN substrate. © *2010 American Institute of Physics*. [doi:10.1063/1.3457783]

Single photon detectors (SPDs) find use in a variety of scientific, military, and civilian applications including free-space optical communication, quantum computing, astrophysics, and biological agent detection.[1] Compared to existing SPDs such as photomultiplier tubes (PMTs), avalanche photodiodes (APDs) presents numerous advantages such as lower operation voltages and much reduced sizes. APDs based on wide band-gap semiconductors are of special interest where there is a need for reliable ultraviolet (UV) detectors. III-nitride-based UV APDs are the most promising candidates to replace conventional PMTs due to the tunability of their band-gap ($3.4<Al_xGa_{1-x}N<6.2$ eV) to cover the entire UV spectrum and their ability to achieve low-noise internal gain.[2–4]

Back-illuminated GaN *p-i-n* diodes benefit from hole-initiated multiplication which yields gain and noise characteristics with superior performances due to the higher hole impact ionization coefficients.[4] Back-illumination also allows easier integration and packaging of APDs through flip-chip bonding technology. However, growing GaN based APDs on conventional UV transparent substrates like sapphire[5–7] results in an effective lattice mismatch as high as 16%, which leads to dislocation densities on the order of 10^9 cm^{-2}.[8] These lattice-mismatch-induced dislocations increase the leakage current, disrupt the electric field distribution, and can result in premature microplasma breakdown—all of which limit the avalanche gain, making the realization of high performance APDs challenging. Low-dislocation density free-standing (FS) GaN substrates are a promising alternative, enabling homoeptaxial growth and yielding significantly lower dislocation density devices. Recently, APDs grown homoepitaxially on FS GaN have shown improved gain performance and yield; however, in spite of the high gain, the single photon detection efficiency (SPDE) of these devices were limited to ~1%.[9]

In this study, we report improved Geiger- and linear-mode operation of front-illuminated GaN APDs, grown on low dislocation density ($<10^6$ cm^{-2}) FS c-plane GaN substrates. The same *p-i-n* structure was also grown on conventional c-plane sapphire substrates, and we study and compare the front- and back-illuminated performance of these APDs.

The *p-i-n* structure was grown in an AIXTRON 200/4-HT horizontal-flow low-pressure metal-organic chemical vapor deposition reactor using trimethylgallium and ammonia (NH_3) as the group-III and group-V sources, respectively. Bis(cyclopentadienyl)magnesium (DCpMg) and silane (SiH_4) were used as a *p*- and *n*-type dopant sources, respectively. In order to improve the crystalline quality and surface morphology, prior to the growth of the APD structure, a 2-μm-thick GaN or 600-nm-thick AlN template layer was grown on the FS-GaN and sapphire substrates, respectively. The APD structure (inset of Fig. 1) is composed of

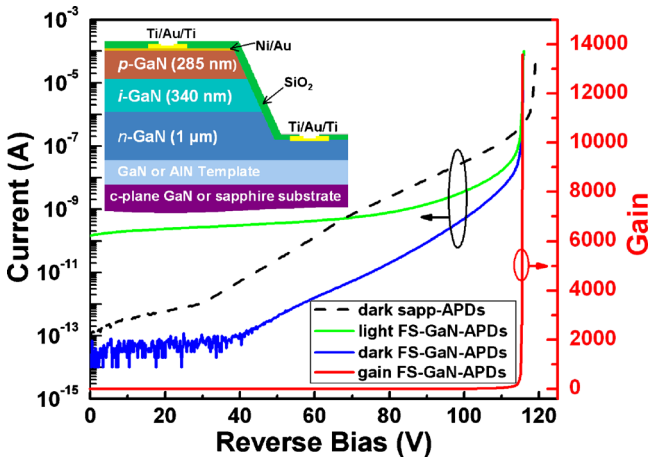

FIG. 1. (Color online) Reverse-bias dark-current characteristics are shown for 225 μm^2 area sapp-APD (dashed line) and dark-current and photocurrent showing maximum gain of 14 000 for FS-GaN-APDs. Dark current and photocurrent are shown on the left axis and gain is shown on the right axis. The inset displays a cross-sectional sketch of the APD.

a)Electronic mail: razeghi@eecs.northwestern.edu.

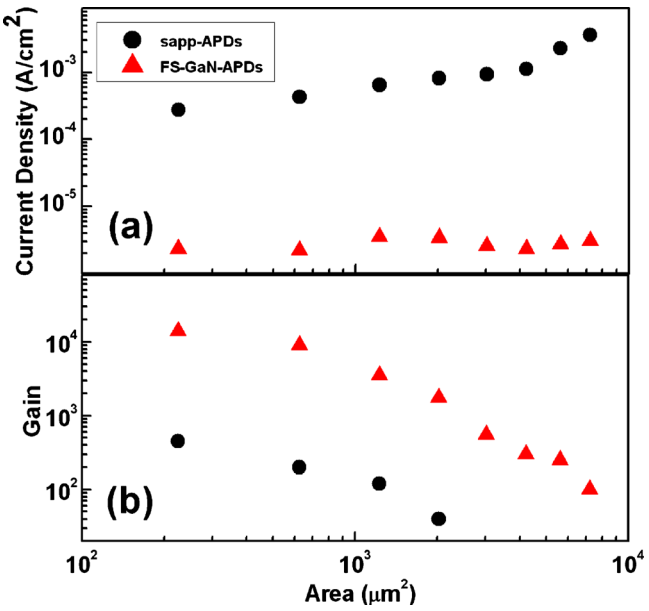

FIG. 2. (Color online) (a) Reverse-bias dark-current density and (b) gain, both as a function of area, are shown for the sapp-APDs and FS-GaN-APDs.

1-μm-thick *n*-type GaN:Si, followed by 340-nm-thick *i*-GaN, and 285-nm-thick *p*-type GaN:Mg layer. The carrier concentrations of these layers were estimated by Hall-effect measurements of test samples grown on AlN template on c-plane sapphire substrates. At room temperature, measurements yielded values of 2.0×10^{15} and 2.0×10^{18} cm^{-3} for the electron concentrations in the *i*-GaN and *n*-GaN layers, respectively and 4.0×10^{17} cm^{-3} for the hole concentration in the *p*-GaN layer. Following the growth, several arrays of 225 to 7225 μm^2 mesa structures were defined via photolithography and dry etching, followed by metal evaporation and SiO_2 passivation. Details of the device fabrication can be found elsewhere.[10]

The electrical properties of the fabricated devices were studied. Figure 1 shows the current-voltage (I-V) characteristics of APDs grown on FS-GaN and c-plane sapphire substrates. The dark current of the FS-GaN-APD remains below the measurement limit up to a reverse bias of ~40 V, for 225 μm^2 area devices, it then increases gradually. Sapphire-APDs (sapp-APDs) have a universally higher dark current. At a reverse bias of 70 V sapp-APDs exhibited a dark current density of 2.7×10^{-4} A/cm^2 whereas FS-GaN-APDs had a lower dark current density of 2.1×10^{-6} A/cm^2. This significantly lower dark current is attributed to the reduced dislocation density in the GaN layers grown homoepitaxialy on the FS-GaN. The current of both devices increases sharply at a reverse bias of 114 V (FS-GaN-APDs) and 117 V (sapp-APDs). The FS-GaN-APDs present a ~1.29 times steeper breakdown than the sapp-APDs, which implies that carriers in the FS-GaN-APDs are statistically more likely to trigger multiplication events and thus higher photon detection efficiency is expected in Geiger-mode operation.

The dark current density at a reverse bias of 70 V was studied for different mesa areas and the results are shown in Fig. 2(a). As the area increases from 225 to 7225 μm^2, sapp-APDs demonstrate an increase in dark current density from 2.7×10^{-4} to 3.6×10^{-3} A/cm^2, whereas for FS-GaN-APDs a negligible difference is observed. The increase in dark current density for sapp-APDs is mainly correlated with higher threading dislocation densities introduced from the lattice-mismatched heterointerfaces.

To study the gain, the APDs were illuminated by a xenon lamp through a UV fiber-optic cable and monochromator set at 340 nm. The sapp-APD structure is suitable for both front- and back-illumination, yielding multiplication dominated by electrons or holes, respectively.[4] However, due to UV absorption in the thick FS GaN substrate, the FS-GaN-APD can only be operated under front-illumination. The gain characteristics were extracted from the photocurrent under reverse bias.[11] Based upon the maximum achievable external quantum efficiency after accounting for reflection and absorption, the gain on-set was determined to be 30 V.[4] The sapp-APDs were tested under both back- and front-illumination, and for a 225 μm^2 device gains of ~450 and 220 were observed, respectively. The same area FS-GaN-APD, under front-illumination, achieved a maximum gain of ~14 000 (Fig. 1). This gain is comparable to other works.[12] In Fig. 2(b), the gains of both sapp-APDs and FS-GaN-APDs are plotted as a function of area. The gain of FS-GaN-APDs decreases from ~14 000 to 150 as the diode area increases from 225 to 7225 μm^2. The main reason is that the dark current increases faster than the current under illumination. The sapp-APDs showed similar gain characteristics; however due to the higher dark current density, the dark current becomes commensurate with the photocurrent for devices larger than 2025 μm^2.

Next, Geiger-mode operation of the APDs was studied. In pulse-gated Geiger-mode detection, the dc reverse bias is kept below the breakdown voltage and the APD is pulsed with an ac-bias pushing the total voltage above the breakdown for a short duration of time.[13] When APDs are biased for Geiger-mode, a single photon with a sufficient energy can trigger a self-sustaining electron-hole multiplication process.[14] Ideally, when there are no photogenerated carrier(s), the APD should not trigger an avalanche response; however, in practice, carriers injected into or thermally generated inside the multiplication region during the ac pulse contribute dark counts. During the avalanche process, carriers can also be trapped in defects. If the subsequent ac-pulse occurs before the decay of the trapped carriers they can retrigger an avalanche; this phenomena is called after-pulsing.[15,16] This effect limits the operation rate for photon counting and degrades the APDs performance. In order to study after-pulsing, a pulse-gated quenching circuit[14] was used. A reverse-dc bias (V_{dc}) was applied to the APD through 46 kΩ load-resistor to keep it at a base-line voltage below breakdown, and an ac-pulse (V_{ac}) was coupled in to the device through a 50 nF capacitor to increase the total voltage above breakdown. A Stanford Research model SR400 gated-photon counter was employed to discriminate the dark counts from photo counts. The gating pulse was chosen as 10 ns and the dead-time between pulses was varied from 5 μs to 1 ms. The FS-GaN- and sapp-APDs both showed a similar decay of the after-pulsing as the dead time was increased; beyond 40 μs both devices were free of after-pulsing. The similar decay rate observed for both APDs implies that the dominant trapping mechanism is independent of the change in substrate-induced defects between the two samples. For subsequent measurements a dead time of 100 μs was used.

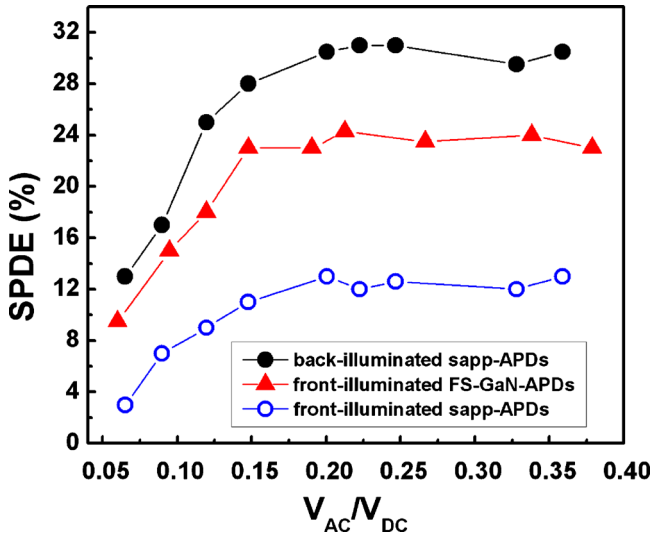

FIG. 3. (Color online) SPDE efficiency is plotted as a function of ac-bias to dc-bias ratio (V_{ac}/V_{dc}) for FS-GaN-APDs (under front-illumination) and sapp-APDs (under front- and back-illumination).

Next, we studied the optimal Geiger-mode operation conditions. As the reverse-dc bias (V_{dc}) was decreased from 110 to 90 V the ac-pulse (V_{ac}) was increased accordingly from 6 to 25 V to keep the total voltage approximately the same. The monochromator was set at 340 nm and the input slit was adjusted to correspond to a photon flux of one photon per pulse. The SPDE as a function of V_{ac}/V_{dc} was investigated for 625 μm^2 area front- and back-illuminated sapp-APDs and front-illuminated FS-GaN-APDs (Fig. 3). The SPDE is a product of the probability that an incident photon will create an electron-hole pair and the probability that the carrier(s) injected into the high field region will trigger an avalanche event. A total voltage ($V_{ac}+V_{dc}$) above breakdown is needed for avalanche breakdown. However, if V_{dc} is only a few volts below breakdown; primary dark carriers can go through a series of impact ionization events with nonself-sustaining but high-average gain before the arrival of pulse. The probability of carriers remaining in the multiplication region when the voltage pulse arrives, becomes higher as V_{dc} gets closer to breakdown. Reducing V_{dc} results in a lower dark count probability (DCP) which is the mainspring of the increase in SPDE for sapp- and FS-GaN-APDs. However, Fig. 3 shows that the SPDE tends to saturate after a certain value of V_{ac}/V_{dc}, this is attributed to the fact that as V_{dc} decreases, trap-assisted tunneling contributes fewer dark counts while thermal generation remains constant in the lower V_{dc} region.[17]

The sapp-APDs under a V_{ac} of 16 V, showed a maximum SPDE of ~13% and 30.5% under front- and back-illumination, respectively, whereas the DCP was measured to be ~0.57. Compared to electron initiated ionization, more than two times higher SPDE was achieved for hole-initiated ionization (back-illumination). Due to optimized Geiger-mode operation conditions, the SPDE value observed for back-illumination is approximately 1.5 times higher than our previous result for similar structure APD grown on sapphire substrates.[14] The FS-GaN-APDs under similar operation conditions (V_{ac}=17 V), showed a maximum SPDE of ~24.3% under front-illumination and a DCP of ~0.41. This SPDE value is significantly higher compared to other SPDE values reported for front-illuminated GaN APDs.[9] Alternately, the discriminator voltage can be set to maximize the SPDE while minimizing the number of spurious dark counts; a SPDE of 8.8% with a DCP of ~0.01 is realized for the FS-GaN-APD.

In summary, Geiger-mode APDs on FS GaN substrates and c-plane sapphire substrates were compared and optimum Geiger-mode operation conditions were studied. Under front-illumination FS-GaN devices showed a maximum SPDE of 24.3% whereas APDs grown on sapphire showed only ~13%. The sapp-APDs was also operated under back-illumination, and yielded a SPDE of ~30.5%; this is attributed to the higher hole ionization coefficients. We believe that by flip-chip bonding the FS-GaN-APDs and performing substrate removal, we can benefit from both the higher hole-ionization coefficient as well as the dislocation reduction.

The authors acknowledge Dr. J. Zavada of ARO, Dr. Stuart Horn of U.S. Army Research Laboratory, Dr. M. Ulmer of Northwestern University Department of Physics and Astronomy for their interest and encouragement, and Mr. Bayram acknowledges Ludo Frevel Crystallography Scholarship.

[1] I. Prochazka, K. Hamal, and B. Sopko, J. Mod. Opt. **51**, 1289 (2004).
[2] E. J. Tarsa, P. Kozodoy, J. Ibbetson, B. P. Keller, G. Parish, and U. Mishra, Appl. Phys. Lett. **77**, 316 (2000).
[3] E. Monroy, F. Calle, J. L. Pau, E. Muñoz, F. Omnès, B. Beaumont, and P. Gibart, J. Cryst. Growth **230**, 537 (2001).
[4] R. McClintock, J. L. Pau, K. Minder, C. Bayram, P. Kung, and M. Razeghi, Appl. Phys. Lett. **90**, 141112 (2007).
[5] S. Verghese, K. A. McIntosh, R. J. Molnar, L. J. Mahoney, R. L. Aggarwal, M. W. Geis, K. M. Molvar, E. K. Duerr, and I. Melngailis, IEEE Electron Device Lett. **48**, 502 (2001).
[6] B. Yang, T. Li, K. Heng, C. Collins, S. Wang, J. C. Carrano, R. D. Dupuis, J. C. Campbell, M. J. Schurman, and I. T. Ferguson, IEEE J. Quantum Electron. **36**, 1389 (2000).
[7] T. Tut, T. Yelboga, E. Ulker, and E. Ozbay, Appl. Phys. Lett. **92**, 103502 (2008).
[8] R. D. Dupuis, J.-H. Ryou, S.-C. Shen, P. D. Yoder, Y. Zhang, H. J. Kim, S. Choi, and Z. Lochner, J. Cryst. Growth **310**, 5217 (2008).
[9] S. Choi, H. J. Kim, Y. Zhang, X. Bai, D. Yoo, J. Limb, J. H. Ryou, S. C. Shen, P. D. Yoder, and R. D. Dupuis, IEEE Photonics Technol. Lett. **21**, 1526 (2009).
[10] K. Minder, J. L. Pau, R. McClintock, P. Kung, C. Bayram, M. Razeghi, and D. Silversmith, Appl. Phys. Lett. **91**, 073513 (2007).
[11] J. L. Pau, C. Bayram, R. McClintock, M. Razeghi, and D. Silversmith, Appl. Phys. Lett. **92**, 101120 (2008).
[12] Y. Zhang, D. Yoo, J.-B. Limb, J.-H. Ryou, R. D. Dupuis, and S.-C. Shen, Phys. Status Solidi **5**, 2290 (2008).
[13] S. Cova, M. Ghioni, A. Lacaita, C. Samori, and F. Zappa, Appl. Opt. **35**, 1956 (1996).
[14] J. L. Pau, R. McClintock, K. Minder, C. Bayram, P. Kung, M. Razeghi, E. Munoz, and D. Silversmith, Appl. Phys. Lett. **91**, 041104 (2007).
[15] Y. Kang, H. X. Lu, Y. H. Lo, D. S. Bethune, and W. P. Risk, Appl. Phys. Lett. **83**, 2955 (2003).
[16] S. Cova, A. Lacaita, and G. Ripamonti, IEEE Electron Device Lett. **12**, 685 (1991).
[17] J. P. Donnelly, E. K. Duerr, K. A. McIntosh, E. A. Dauler, D. C. Oakley, S. H. Groves, C. J. Vineis, L. J. Mahoney, K. M. Molvar, P. I. Hopman, K. E. Jensen, G. M. Smith, S. Verghese, and D. C. Shaver, IEEE J. Quantum Electron. **42**, 797 (2006).